SIDEROPHILE ELEMENTS IN METAL FROM NORTHWEST AFRICA 2526, AN ENSTATITE CHONDRITE PARTIAL MELT RESIDUE. M. Humayun[1], K. Keil[2] and A. Bischoff[3], [1]National High Magnetic Field Laboratory & Dept. of Geological Sciences, Florida State University, Tallahassee, FL 32310, USA (humayun@magnet.fsu.edu), [2]Hawai'i Institute of Geophysics and Planetology, School of Ocean and Earth Science and Technology, University of Hawai'i at Manoa, Honolulu, Hawai'i 96822, USA (keil@hawaii.edu), [3]Institut für Planetologie, Westfälische Wilhelms-Universität, 48149 Münster, Germany (bischoa@uni-muenster.de).

Introduction: Enstatite-rich meteorites form a distinct clan characterized by an extremely reduced mineralogy [1], and identical oxygen isotope compositions [2]. Among the diverse meteorites that share these characteristics are the EH and EL chondrites, aubrites, anomalous iron meteorites (Horse Creek, Mt. Egerton, LEW 85369), various impact-melt meteorites of enstatite chondrite parentage, including Zaklodzie [3, 4, 5], and metal-rich enstatite meteorites that [3] interpret as partial melt residues of enstatite chondrite parent lithologies, including Itqiy and NWA 2526. The role of nebular versus planetary processes in the chemical and textural evolution of enstatite chondrites have long been debated [1]. Recent studies of metal in EL3 chondrites reveals the ubiquitous role of impact melting in even the most primitive EL chondrites [6]. New siderophile element data confirm that metal-kamacite associations in EL3s represent injected impact melts [6]. To explore the nature of residual metal in bodies of enstatite chondritic composition, we analyzed metal in NWA 2526 for siderophile element composition by laser ablation ICP-MS. NWA 2526 is a coarse-grained rock dominated by equigranular grains of enstatite (~85 vol. %) with 10-15 vol. % of large kamacite grains + terrestrial weathering products, lacks plagioclase, and contains <1% sulfides [3]. NWA 2526 is argued to represent the residue after about 20% partial melt extraction of metallic-sulfide and silicate melts from a body of E chondritic composition [3].

Sample and Analytical Methods: Thin section PL06056 contained five large (mm-sized) metal grains, three of which (grains 1-3) were closely associated and possibly interconnected. Petrographic details have been given elsewhere [3]. Laser ablation ICP-MS analyses were performed at Florida State University using a New Wave UP213 laser ablation system coupled to a Finnigan Element1, details of which have been provided elsewhere [7]. Metal grains were analyzed with a line scan using a 25 µm spot size, 5 µm/s scan speed, 10 Hz repetition rate, 100% power output (0.075 mJ). The peaks ^{29}Si, ^{31}P, ^{34}S, ^{53}Cr, ^{57}Fe, ^{59}Co, ^{60}Ni, ^{63}Cu, ^{69}Ga, ^{74}Ge, ^{75}As, ^{97}Mo, ^{102}Ru, ^{103}Rh, ^{106}Pd, ^{120}Sn, ^{121}Sb, ^{182}W, ^{185}Re, ^{192}Os, ^{193}Ir, ^{195}Pt, and ^{197}Au, were acquired by line scans in low resolution mode. Standards used included North Chile (Filomena) IIA iron meteorite, Hoba IVB iron meteorite, and NIST SRM 1263a steel. Abundances for standards are from [8], except for Hoba [9].

Results: Siderophile element concentrations are homogeneous within each grain across ~ 1 mm. Metal compositions for the five grains represent averages taken over the interior of each grain, and are close enough in composition (±10%) that the metal in NWA 2526 can be represented by a single average of the five grains. Grains #4 and #5 exhibit resolvable variations in the most compatible siderophile elements (Re, Os, Ir) of about 10% relative to the average of NWA 2526 metal.

The Si (4.56±0.18 wt %) and P (~950 ppm) contents of the metal are similar to those determined by electron microprobe [3]. The S (200-500 ppm) and Cr (30-45 ppm) contents are low. The siderophile element abundances are shown in Fig. 1 on a CI-chondrite and Ni-normalized basis. Also shown are bulk metal separates from EH and EL chondrites [10].

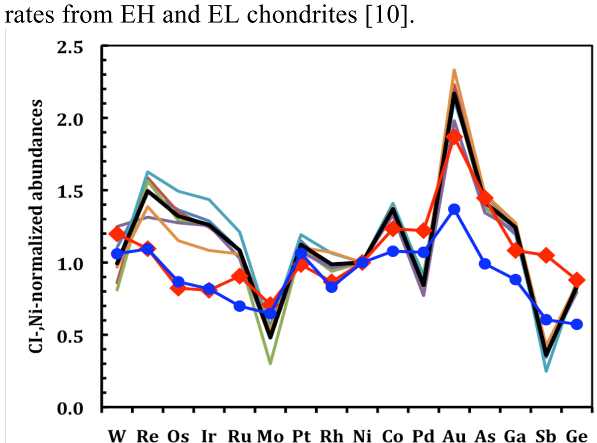

Fig. 1: CI-, Ni-normalized elemental abundances for NWA 2526 metal, and separated metal from EH (red diamonds) and EL (blue circles) chondrites [10].

Many of the characteristic features of enstatite chondrite metal are exhibited by NWA 2526 metal, including the large positive Au and As anomalies, the high Co/Ni ratio, and the negative Mo anomaly. NWA 2526 metal has higher relative abundances of Re, Os, and Ir, and lower Pd than bulk metal separates from EH or EL chondrites. These variations are consistent with an origin of NWA 2526 metal as a partial melt residue of enstatite chondrite parentage, as previously argued by [3], since Re, Os, and Ir are the most compatible elements during partial melting of both S-bearing or C-bearing metallic liquids [11, 12]. By contrast, Pd is incompatible in solid metal for low contents of C and S in metallic liquids [11, 12]. The low W/Re ratio in NWA 2526 metal requires the presence of a C-rich metallic liquid, since W is compatible in S-bearing liquids, but becomes incompatible in C-bearing liquids [12].

Discussion: Experimental partial melting of the Indarch enstatite chondrite revealed that there are three co-existing, immiscible metallic liquids produced: a S-rich liquid, a C-rich liquid, and a Si-rich liquid [13]. Experimental studies of siderophile element partitioning for S- and C-bearing metallic liquids are currently available [11, 12], but not for Si-bearing metallic liquids, which adds a measure of ambiguity to our interpretations of the origin of NWA 2526 metal. In general, the addition of C, P, and S, to metallic liquids drives most siderophile elements to become increasingly compatible with increasing alloying of non-metallic constitutents, with the notable exception of elements that form stable carbides (Cr, Mo, W, Re) [12]. This may also be expected for Si-bearing liquids, with the important exception again of any elements that form stable silicides (e.g., Ni), although little is known about silicides beyond the tendency of Ni to form perryite. Fig. 2 compares the compositions of solid metal in equilibrium with S-bearing and C-bearing metallic liquids. With the exception of Au and As abundances, all elemental abundances plot intermediate between these two compositions. No match to the abundance pattern was found for either end-member liquid. Neither C- nor S-bearing melts can account for the compatible behavior of As, or to a lesser extent Au, in NWA 2526 metal.

Comparison with Si-bearing iron meteorites. In Fig. 3, the composition of NWA 2526 metal is compared with elemental abundances for Si-bearing iron meteorites, including Horse Creek, Mount Egerton, and LEW 85369. Also shown is the average metal composition of Norton County aubrite [5]. The match between LEW 85369, Mount Egerton, and NWA 2526 metal, is close with the exception of the Ni/Co ratio. For Horse Creek and Norton County metal, the mismatch in Re is prominent. However, the compositional similarities indicate that all of these meteorites are genetically related. This does not imply that these meteorites are derived from a single parent body, but does require that the meteorites are all derived from material of similar composition.

Conclusions: NWA 2526 metal represents residual metal after partial melting of an enstatite chondrite parent lithology, confirming the interpretations of an earlier petrological study [3]. The metallic melts removed included both C- and S- (and perhaps Si-) bearing liquids. Compositionally, NWA 2526 metal provides a chemical link to to Si-bearing iron meteorites.

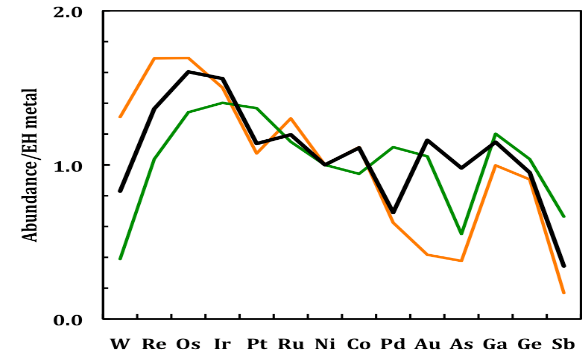

Fig. 2: Elemental abundance of NWA 2526 metal (black) normalized to Ni and bulk EH metal [10], with results of partial melting models involving (a) removal of 60% S-rich metallic liquid (orange), and (b) removal of 40% C-rich metallic liquid (green).

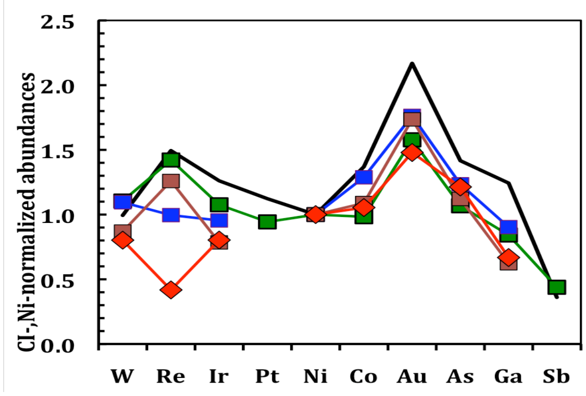

Fig. 3: Comparison of compositions of NWA 2526 metal (black line) with Si-rich iron meteorites (Horse Creek: blue squares [15]; Mount Egerton [15]: brown squares; LEW 85369: green squares [14]), and Norton County (aubrite) metal: red diamonds [5].

References: [1] Keil K. (1989) *Meteoritics, 24*, 195-208. [2] Clayton R. N. and Mayeda T. K. (1996) *GCA, 60,* 1999-2017. [3] Keil K. and Bischoff A. (2008) *MAPS, 43,* 1233–1240. [4] McCoy T. J. et al. (1995) *GCA, 59,* 161-175. [5] Casanova I. et al. (1993) *GCA, 57*, 675-682. [6] Van Niekirk D. L. et al. (2009) *LPSC XL,* (this volume). [7] Humayun M. et al. (2007) *GCA, 71*, 4609-4627. [8] Campbell A. J. et al. (2002) *GCA, 66*, 647-660. [9] Walker R. J. et al. (2008) *GCA, 72*, 2198-2216. [10] Kong P. et al. (1997) *GCA, 61*, 4895-4914. [11] Chabot N. L. et al. (2003) *MAPS, 38*, 181-196. [12] Chabot N. L. et al. (2006) GCA, 70, 1322-1335. [13] McCoy T. J. et al. (1999) *MAPS, 34,* 735-746. [14] Wasson J. T. (1990) *Science, 249*, 900-902. [15] Malvin D. J. et al. (1984) *GCA, 48*, 785-804.